Inhibition of vimentin or B1 integrin reverts morphology of prostate tumor cells grown in laminin-rich extracellular matrix gels and reduces tumor growth *in vivo*

Xueping Zhang,[1] Marcia V. Fournier,[4] Joy L. Ware,[2] Mina J. Bissell,[4] Adly Yacoub,[3] and Zendra E. Zehner[1]

Departments of [1]Biochemistry and Molecular Biology, [2]Pathology, [3]Radiation Oncology and Massey Cancer Center, Virginia Commonwealth University-Medical Campus, Richmond, Virginia and [4]Life Sciences Division, Lawrence Berkeley National Laboratory, Berkeley, California

Requests for Reprint:

Zendra E. Zehner
Department of Biochemistry and Molecular Biology
Virginia Commonwealth University-Medical Campus
P.O. Box 980614, Richmond, VA 23298-0614.
Phone: 804-828-8753
Fax: 804-828-1473
E-mail: zezehner@vcu.edu

LBNL/DOE funding & contract number: DE-AC02-05CH11231

Abstract

Prostate epithelial cells grown embedded in laminin-rich extracellular matrix (lrECM) undergo morphologic changes that closely resemble their architecture *in vivo*. In this study, growth characteristics of three human prostate epithelial sublines derived from the same cellular lineage, but displaying different tumorigenic and metastatic properties *in vivo*, were assessed in three-dimensional lrECM gels. M12, a highly tumorigenic and metastatic subline, was derived from the immortalized, prostate epithelial P69 cell line by selection in athymic, nude mice and found to contain a deletion of 19p-q13.1. The stable reintroduction of an intact human chromosome 19 into M12 resulted in a poorly tumorigenic subline, designated F6. When embedded in lrECM gels, the parental, nontumorigenic P69 line produced acini with clearly defined lumena. Immunostaining with antibodies to β-catenin, E-cadherin, or α_6 and β_1 integrins showed polarization typical of glandular epithelium. In contrast, the metastatic M12 subline produced highly disorganized cells with no evidence of polarization. The F6 subline reverted to acini-like structures exhibiting basal polarity marked with integrins. Reducing either vimentin levels via small interfering RNA interference or the expression of α_6 and β_1 integrins by the addition of blocking antibodies, reorganized the M12 subline into forming polarized acini. The loss of vimentin significantly reduced M12-Vim tumor growth when assessed by s.c. injection in athymic mice. Thus, tumorigenicity *in vivo* correlated with disorganized growth in three-dimensional lrECM gels. These studies suggest that the levels of vimentin and β_1 integrin play a key role in the homeostasis of the normal acinus in prostate and that their dysregulation may lead to tumorigenesis. [Mol Cancer Ther 2009;8(3):499–508]

Introduction

The extracellular environment is essential for establishing and maintaining cell differentiation during glandular morphogenesis (1). In the developing prostate, budding urogenital epithelial cells attach to the extracellular matrix (ECM) through integrin receptors and migrate into the mesenchyme to form acini containing lumen and displaying polarity (2). Integrins play an important role in maintaining the bidirectional communication between prostate cells and the ECM. Moreover, their expression patterns are known to change during tumor progression; for example, β_1 integrin levels increase, whereas β_2 and β_3 integrins remain unchanged (3). Differential expression of α_6 and α_3 integrins suggests a reorganization of adhesion complexes during prostate cancer progression (4). Because α_6 β_1 integrin is one leading component of these complexes, it was proposed that inhibition of either α_6 or β_1 integrin might reverse the invasive phenotype (5). Tumor stromal interactions have also been found to influence prostate cancer progression (6). Abnormal stroma containing cancer-associated fibroblasts promoted carcinogenesis of nontumorigenic, genetically abnormal epithelial cells but had no effect on normal epithelial cells. Growth of cells in threedimensional environments, which better mimic the normal cellular microenvironment, offers unique approaches for elucidating signals that contribute to tumor progression *in vivo* (7).

Prostate tumors display a loss of the epithelial marker E-cadherin and a switch in intermediate filament protein (IFP) expression from keratins to vimentin, resulting in the loss of hemidesmosomes (5). This switch in expression may earmark cells that have undergone an epithelial to mesenchymal transition. In cancer, the epithelial to mesenchymal transition may be a step toward tumor invasion, although this hypothesis remains controversial (8–10). Nonetheless, a role for vimentin in motility has been well documented in several cell types and may be important in cancer where motility is one component required to establishing a metastatic phenotype. Motility and migration of breast, head and neck, or colon cancer cells were markedly affected by vimentin RNA interference (11–14, 38, 39). Although extensive studies are lacking in prostate, the expression of vimentin may be an underappreciated component of prostate tumor growth and progression.

Normal methods for culturing cells on plastic tissue culture dishes, called two-dimensional, do not duplicate the natural milieu surrounding epithelial cells *in vivo* nor do they produce polarized acini surrounded by basement membrane, as found in normal prostate tissue (15). To alleviate this problem, epithelial cells have been cultured three-dimensionally in laminin-rich ECM (lrECM) gels (16). Because cells grown in lrECM gels closely duplicate glandular phenotypic characteristics, these cultures enable an investigation into the influence of ECM and stroma on cell growth and differentiation *in vitro* (5, 16, 17). In the case of prostate epithelial, a variety of different morphologic structures have been obtained depending on cell type and culture conditions. For example, RWPE-1, an immortalized, nontumorigenic prostate epithelial cell line, was

able to migrate into, and form branches terminating in, acini when plated on top of lrECM gels (2). However, NMU-transformed RWPE-1 cells formed solid cell masses (18).Cultures of RWPE-2, a Ki-ras-transformed subline of RWPE-1, resulted in single to small clumps of cells with no evidence of acinus organization. The unrelated human prostatic carcinoma cell lines DU-145, PC3, or PNTC-C2 formed amorphous balls called spheroids without organization or lumen (2, 19). These different results could be due to the comparison of genetically dissimilar cell lines or related sublines, which were plated on top of lrECM gels rather than embedded. Due to these inconsistent results, we initiated a more thorough analysis of the morphologic structures formed by a unique set of genetically related, malignant or nonmalignant prostate sublines grown embedded in lrECM gels.

P69 is an immortalized, nonmetastatic prostate epithelial cell line (20). A metastatic subline M12 was derived by *in vivo* selection (three passages) of P69 cells in male, athymic nude mice (21). Analysis of M12 chromosomal alterations detected a novel 16:19 unbalanced translocation resulting in the deletion of one copy of 19p-q13.1. Microcell-mediated chromosome transfer restored an intact, neomycin-marked human chromosome 19 to generate the F6 subline (22). The M12 subline is fast growing and highly metastatic on orthotopic injection in athymic, nude mice, whereas the F6 subline is slow growing, barely forms small tumors, and is not metastatic. These related sublines present an excellent model for investigating requirements for prostate cancer tumor progression.

The behavior of the P69, M12, and F6 human prostate epithelial sublines was analyzed in three-dimensional cultures and compared with the LNCaP and PC3 cell lines. Under these conditions, we found distinct differences in their morphologic properties, which correlated with their behavior *in vivo*. The addition of blocking antibodies to α_6 or β_1 integrin or the stable repression of vimentin expression via short hairpin RNA (shRNA) technologies enabled the highly tumorigenic, metastatic M12 cells to form organized acini structures akin to those formed by the P69 and F6 sublines.

Materials and Methods

Substrates and Antibodies

Commercially prepared EHS ECM extract, growth factor reduced, lrECM (Cultrex BME) was used for three dimensional cultures (23). Antibodies used for Western blotting and immunostaining studies were as follows: androgen receptor (sc-7305; Santa Cruz Biotechnology), E-cadherin (U3254; Sigma), β-catenin (H-102; Santa Cruz Biotechnology), keratin 5/6 (DAKO), keratin 8 (ab9287; Abcam), β_1 integrin (MAB1951Z; Chemicon), α_6 integrin (MAB1378; Chemicon), Ki-67 (clone MIB; Jackson ImmunoResearch Laboratories), vimentin (V6630; Sigma), and β-actin (A5441; Sigma). FITC-conjugated anti-rat IgG was from Jackson ImmunoResearch Laboratories, whereas fluorescent Alexa 488/546-labeled anti-rabbit and mouse IgG were from Invitrogen. Blocking antibodies for β_1 integrin (AIIB2), originally a gift from C. Damsky, was isolated and prepared from a hybridoma cell line (Sierra Biosources), whereas α_6

integrin blocking antibody (GoH3) was from BD Pharmingen. Nonspecific rat and mouse IgG and horseradish peroxidase-conjugated secondary antibodies were from Santa Cruz Biotechnology. Goat F(ab¶)2 anti-mouse IgG was from Invitrogen (MAB35000).

Cell Culture and Stable Transfectants

The establishment, maintenance, and characterization of the SV40 T antigen-immortalized human prostate epithelial cell sublines P69, M12, and F6 have been described previously (21, 22, 24). M12 cells were stably transfected with a plasmid psiREN-RetroQ (BD Biosciences) expressing a human vimentin shRNA (M12-Vim) of sequence 5'-ATCCGCACCGAGTTCAAGAACACCTTTTCAAGAGAGGTGTTCTTGAACTCGGTGTTCTTTTTTTCTAGAG-3' (the human vimentin gene sequence is italicized) as described previously (14). M12 cells transfected with either empty psiREN-RetroQ vector (M12+siREN) or vector containing a nontargeting control sequence (M12+NTC: 5'-GATCCGGCATGTACTAGCCTAAGCGTTTTCAAGAAGACGCTTAGGCTAGTACATGC-TTCTTTTTTTCTAGAG-3') served as negative controls. A search of the human genome or Sanger microRNA database confirmed no significant match to the nontargeting control sequence. Cells were transfected using TransIT-LT1 transfection reagent (Mirus Bio) according to the manufacturer's instructions. Puromycin-resistant cells were selected in 400 ng/mL puromycin and maintained in 100 ng/mL (Amersham Biosciences). The down-regulation of vimentin gene expression in stable transformants designated as M12-Vim was confirmed by Western blot analysis. LNCaP cells were cultured in RPMI 1640 plus 10% fetal bovine serum and 1% penicillin/streptomycin (25). PC3 cells were retrieved from tumors grown in athymic mice andmaintained in RPMI 1640 for five passages before embedding in lrECMas described previously (25).

Acinar Morphogenesis

Three-dimensional cultures were prepared by growing prostate cancer cells to 80% confluence of monolayer on plastic tissue culture dishes followed by trypsinization and collection by centrifugation. lrECM was prethawed on ice overnight. Cells (1×10^6) were mixed with 1 mL undiluted lrECM and added to each well of a 6-well dish. Following incubation for 1 h at 37°C, the lrECM had polymerized. Medium (3 mL) containing a specific drug, if needed as cited above, was added on top of the solidified lrECM-cell mix. The same batch of lrECM was used throughout this study. Medium was replaced every other day and cultures were grown for up to 16 days in lrECM, maintaining their organization for this entire period.

***In vivo* Tumorigenicity Assays**

Tumorigenicity of M12 cells stably transformed with the vimentin shRNA expression plasmid (M12-Vim), vector alone (M12+siREN), or vector expressing the nontargeting RNA control (M12+NTC) was assessed by s.c. injection of 1×10^6 cells into male, athymic nude mice as described previously (21). A total of 15 mice were injected as

follows: 6 mice with M12-Vim, 4 mice with M12+siREN, and 5 mice with M12+NTC for a total of 9 mice serving as negative controls. Tumor growth was monitored by caliper measurement for up to 42 days and approximate tumor volume (mm^3) was calculated as length _ $width^2$ / 2. At the time of euthanasia, tumors were removed and samples were fixed in 10% buffered formalin, paraffin-embedded, stained, and examined for vimentin expression. All experiments were conducted under a protocol approved by the Institution Animal Care and Use Committee of Virginia Commonwealth University.

Western Immunoblotting

Harvested cells were washed with cold 1x PBS and then lysed in 4% SDS in 1x PBS with protease inhibitor cocktail (Sigma). After brief sonication, an equal volume of 1x PBS was added to reduce the SDS concentration to 2%. Lysates were then centrifuged for 10 min at high speed, supernatants were collected, and protein concentration was measured using the Bio-Rad D_c Protein Assay kit. Equivalent amounts of protein (40 μg) were boiled in 1x SDS sample buffer for 5 min and analyzed on 8% to 16% gradient polyacrylamide gels (NuSep). Western immunoblot analysis was done and quantified as described previously (26).

Morphologic structures from the various P69-derived cells grown in lrECM gels were harvested as described (23). Cells were transferred to a 50 mL centrifuge tube with 10 mL of 0.5% Na2EDTA in 1x PBS plus 1% protease inhibitor cocktail. The mixture was shaken on ice for 1 h to completely dissolve the lrECM gel, after which cells were collected at 1,000 rpm for 5 min, washed twice with 1x PBS plus protease inhibitor cocktail, and stored at -80ºC. Cell extracts were prepared and Western immunoblot analysis was done as described previously (26).

Indirect Immunofluorescence

A sample (≈10 AL) of lrECM culture was spread on each well of a 4-well chamber slide, air dried, and fixed in 1:1 methanol/acetone at 20ºC for 10 min. The slides were washed by 1x PBS briefly followed by 400 μL of 1x IF buffer (130 mmol/L NaCl, 7 mmol/L Na2HPO4, 3.5 mmol/L NaH2PO4, 7.7 mmol/L NaN3, 0.1% bovine serum albumin, 0.2% Triton X-100, 0.05% Tween 20) with 10% goat serum and a secondary blocking in 200 μL of 1x IF buffer with 10% goat serum and 20 μg/mL goat anti-mouse $F(ab')_2$ fragment for 1 h sequentially. Slides were incubated with primary antibody overnight at 4ºC followed directly by either FITC or Alexa-conjugated secondary antibody (1:200) for 45 min. The dilutions of antibodies used were as follows: α_6 integrin (1:100), androgen receptor (1:50), β catenin (1:100-1:200), β_1 integrin (1:100), keratin 5/6 (1:200), keratin 8 (1:100), E-cadherin (1:200), vimentin (1:200), and Ki-67 (1:200). Nuclei were counterstained with 4',6-diamidino-2-phenylindole (Sigma) overnight at room temperature. Control slides were stained with secondary antibody only. Slides were visualized under a LZM5100 confocal microscope according to the manufacturer's instructions. Representative pictures were shown from experiments repeated at least twice with 20 to 50 morphologic structures analyzed.

Reversion Assay

Equal densities of cells were seeded in lrECM gels containing AIIB2 (160 μg/mL), GoH3 (5 μg/mL), DMSO only, or IgG (5 μg/mL) as negative controls. After 10 days, cells were photographed and stained with specific antibodies as discussed above.

Statistical Analyses

Data are presented as mean $\pm$ SE. A regression model was done to validate significant differences. Statistical analysis used JMP statistical software with significance set at a probability of ≤ 0.05. Where indicated, immunofluorescence staining was quantitated using image J software (NIH). For example, in compiling data for Table 1, an average value was generated from the quantification of four arbitrary sections of each morphologic structure shown in Fig. 2 and compared across panels (d_1-d_4) to generate an arbitrary scale of +++ to -.

Results

Morphologic Properties of P69, M12, and F6 Sublines Grown Embedded in lrECM Gels

When grown on plastic tissue culture dishes (two-dimensional), the cellular morphology of the P69-derived prostate cell sublines is indistinguishable (Fig. 1A, top row). However, when grown embedded (three-dimensionally) in lrECMgels, these genetically similar sublines organize into distinct, different morphologic structures (Fig. 1A, bottom row, and Fig. 2). The nontumorigenic P69 epithelial cell line forms acini (Fig. 1A, lane 1). Although the highly metastatic M12 subline initially forms solid balls of cells called spheroids,within 48 h, the cells began to migrate out of these structures and ultimately penetrate throughout the lrECM gel (Fig. 1A, lane 2). The poorly tumorigenic F6 subline reverted back to forming acini (Fig. 1A, lane 3).

A proteomic analysis of these sublines revealed a notable difference in the expression of the mesenchymal IFP, vimentin (24). Epithelial cells grown on plastic dishes often aberrantly express vimentin (Fig. 1B, top row) albeit at a low level compared with the usual epithelial keratins (27). When grown three-dimensionally, vimentin is not expressed in the P69 subline akin to expression patterns *in vivo* (Fig. 1B, bottom row). Similar to most, if not all, metastatic cancers, vimentin is highly expressed in the metastatic M12 subline grown either two-dimensionally or three-dimensionally (28). Conversely, the amount of vimentin protein is severely reduced in the F6 subline grown under either condition (24). Thus, in both cases, the M12 subline highly expresses vimentin, whereas the P69 and F6 sublines either do not or exhibit a marked decrease in vimentin expression when grown in lrECM gels.

Blocking Vimentin via shRNA Interference Causes a Dramatic Change in the *In vitro* Phenotype of M12 Cells

Previous studies of nonisogenic breast cancer cell lines suggested that vimentin expression is essential but not sufficient to cause tumor metastasis (29). In these prostate sublines, there is a tremendous difference in vimentin expression (24). To determine if vimentin content could have a direct effect on the morphology of the M12 subline, M12s were stably transformed with a vimentin shRNAproducing plasmid called M12-Vim. When grown either two-dimensionally or three-dimensionally, the level of vimentin protein was repressed 85% compared with the wild-type M12 (Fig. 1B). When grown two-dimensionally, there was no apparent difference between the morphology of the M12 and M12-Vim sublines (Fig. 1A, top row). However, when grown three-dimensionally, the M12-Vim subline reverted to acini-like structures (Fig. 1B, bottom row).

Phenotypic Characteristics of P69, M12, and F6, and M12-Vim Grown in lrECm

The parental P69 subline forms smooth, regular acini when grown in lrECM gels (Fig. 2A). Confocal microscopy of a series of pictures taken at a fixed plane through an acinus (Z-stack) and immunostained with α_6 integrin confirms the multicellular nature of these acini with a notable, clear lumen. The similarity of these structures to those formed by prostate glandular epithelium embedded in a matrix of stromal cells was readily apparent (2).

Immunostaining for a variety of relevant IFPs, nuclear, membrane, and cell-surface proteins was used to access protein organization within the morphologic structures formed by these sublines in lrECM gels (Fig. 2B and C). Staining for Ki-67 revealed that nuclei were actively dividing at day 8 for all sublines (Fig. 2B, a_1-a_4). P69 acini did not express vimentin (Fig. 2B, a_1) but did contain β-catenin (Fig. 2B, b_1), E-cadherin (Fig. 2B, c_1), keratin 5/6 (Fig. 2B, d_1), keratin 8 (Fig. 2B, e_1), and α_6 β_1 integrin (Fig. 2C, h_1 and j_1) akin to normal prostate epithelial cells. The overlay (Fig. 2C, k_1) indicated that α_6 β_1 integrin was colocalized and polarized on the outside edge of the acinus as seen in prostate tissue (5, 30). In contrast, by day 8, most of the metastatic M12 subline had grown out of spheroids (Fig. 2B, a_2-e_2 and Fig. 2C, h_2 and j_2). β-Catenin staining of cell-cell junctions confirmed that these cellular masses were not organized into lumen-containing acini (Fig. 2B, b_2). In addition, there was a loss of expression ($\approx$99%) of the epithelial cell marker, E-cadherin (Fig. 2B, c_2), coincident with the emergence of vimentin (Fig. 2B, a_2) as seen in Fig. 1B. Moreover, the M12 cellular mass showed little organization and a loss of polarization as verified by diffuse staining with antibodies to α_6 and β_1 integrins (Fig. 2C, h_2-k_2). In addition, expression of keratin 5/6 was barely detectable (Fig. 2B, d_2), whereas keratin 8 (Fig. 2B, e_2) remained consistent. In a time-course study, it was evident that the M12 subline did initially try to form spheroids (a remnant of one is seen in Fig. 2B, a_2, white arrow), but by day 8 most cells had migrated out of spheroids into the surrounding matrix.

Interestingly, F6 cells with a restored second copy of chromosome 19 produced acini-like structures with a defined lumen (Fig. 2B and C). Expression of vimentin was greatly

reduced (Fig. 2B, a_3) and expression of E-cadherin returned (Fig. 2B, c_3) as well as keratin 5/6 (Fig. 2B, d_3) with the multicellular nature of these acini confirmed by β-catenin staining of cell junctions (Fig. 2B, b_3). Keratin 8 (Fig. 2B, e_3) expression continued. Moreover, F6 acini exhibit α_6 and β_1 integrin polarization with colocalization (note overlay) of α_6 β_1 integrin dimmers (Fig. 2C, h_3-k_3).

Reducing vimentin expression via shRNA also reverted M12 cells back to acini-like structures (Fig. 2B and C). Immunostaining with antibodies to vimentin and E-cadherin showed that the M12-Vim subline expressed Ecadherin and keratin 5/6 instead of vimentin (Fig. 2B, compare c_4 and d_4 with a_4). Western blots confirmed that P69, F6, or M12-Vim acini grown in lrECM gels (threedimensional) retained E-cadherin expression, whereas it was lost (99%) in the M12 subline (data not shown). Again, keratin 8 (Fig. 2B, e_4) remained. M12-Vim cells exhibit polarization of α_6 or β_1 integrins and renewed colocalization of α_6 β_1 integrin dimers (Fig. 2C, h_4-k_4), which is similar to that seen in the P69 or F6 acini (Fig. 2C, k_1 and k_3). Because staining for androgen receptor was negative, in both Western blots of two-dimensional cultures (31) and immunofluorescence staining of three-dimensional structures, pictures are not shown.

Growth of these genetically related sublines was compared with the more familiar prostate cell lines, LNCaP and PC3 (Fig. 2D). Only immunofluorescence staining for proteins relevant to morphologic organization is shown. Both cell lines formed multicellular spheroids with no evidence of a lumen on Z-stack analysis. The least tumorigenic LNCaP cell lines (androgen receptor positive) displayed colocalization and polarization of α_6 β_1 integrins akin to the F6 subline (overlay m_3). However, the highly metastatic PC3 cell line did not exhibit integrin polarization and staining was diffuse (overlay n_3) as in the M12 subline (Fig. 2C, k_2).

Measurement of the P69, F6, and M12-Vim Acini Grown in lrECM

Next, we compared the growth properties of P69, F6, and M12-Vim structures overtime in three-dimensional culture to determine if acini reach a maximum cell number and size, become growth arrested, or maintain a lumen (Fig. 3). Counting the number of nuclei in 100 P69, F6, and M12-Vim acini indicated that these cells were still actively dividing by day 13 in culture (Fig. 3A). Growth arrest occurred around day 16 as confirmed by negative staining for Ki-67 at day 16 compared with day 13 (data not shown). The size of the acini (μm) also reached a maximal level by day 16, consistent with the cell number count per acinus (Fig. 3B). In contrast, M12 sublines still showed positive Ki-67 staining up to day 16. These cultures could not be analyzed past 16 days, as the ability of the lrECM gel to support growth became rate limiting. Because M12 cells form a nonorganized cellular mass rather than acini, it was not relevant to count nuclei. Data were analyzed by regression model with P values of 0.15 and 0.08 (both >0.05) for cell number (Fig. 3A) and acini size (Fig. 3B), which indicates that there is no significant difference among the three sublines.

Blocking Vimentin Expression in M12 Cells Affects Tumor Formation in Nude, Athymic Mice

Previously, the tumorigenicity of the M12 and F6 subline was determined by s.c. injection into male, athymic, nude mice (21). All mice (13 of 13) injected with M12 cells developed tumors after 9 to 15 days. Mice injected with F6 cells either failed to produce tumors (9 of 15) or produced only small tumors (6 of 15) after 120 days. When grown three-dimensionally, reducing the expression of vimentin reverted the M12 cells back to acini-like structures. Next, we asked if the dramatic morphologic difference observed *in vitro* would correlate to tumor growth *in vivo*. To answer this question, tumor formation was assessed by s.c. injection into male, athymic, nude mice of M12 cells stably transformed with vector only (M12+siREN), vector expressing a nontargeting, scrambled RNA sequence (M12+NTC), or M12-Vim (Fig. 4A). By 42 days, 6 of 6 mice injected with M12-Vim displayed tumors, which were >8-fold reduced in size compared with the average of the 9 mice injected with either M12+siREN-or M12+NTC-negative controls. Importantly, there was little difference in the proliferation rate of the M12-Vim subline compared with the negative control cells in two-dimensional culture (data not shown). Thus, the lack of vimentin is not influencing cell growth rate *in vitro*. Regression model analyses using the LSmeans Tukey's honestly significant difference test indicated that there was a significant difference between M12+NTC or M12+siREN and M12-Vim with P values < 0.001. At the completion of the experiment, animals were euthanized, tumors were removed, and continued vimentin expression in the M12+siREN-negative control was verified by immunofluorescence staining (Fig. 4B, right). Little vimentin could be detected in the small tumors formed by the M12-Vim subline (Fig. 4B, left) in agreement with Western blots (Fig. 1).

A comparison of the morphologic properties of these cells *in vitro* and *in vivo* is compiled in Table 1. Tumorigenicity of the original M12 and F6 sublines was documented previously (22). Here, the reduction of vimentin expression in the M12-Vim cells reduced tumor growth compared with the M12 control cells. A reduction in expression of E-cadherin concomitant with activation of vimentin expression is indicative of cells that have progressed through the epithelial to mesenchymal transition (8). It would appear that this transition is occurring in these genetically related sublines when grown embedded in lrECM gels. Coexpression of keratin 5/6 and keratin 8 plus p63 (data not shown) suggests that parental P69 cells were derived from an intermediate cell, proposed to be the progenitor cell of prostate cancer (32) Moreover, the lack of keratin 5 expression in the highly tumorigenic, metastatic, M12 subline is consistent with loss of keratin 5 expression in human prostate cancer metastases (33–35). Overall, these comparisons support the conclusion that the growth of these uniquely related prostate sublines in three-dimensional culture closely parallels their properties *in vivo* and those of glandular epithelium as cells progress to tumor formation and ultimately metastatic prostate carcinoma.

Inhibiting α_6 or β_1 Integrin Activity Can Cause a Phenotypic Reversion

The inclusion of blocking antibodies for β_1 integrin (AIIB2) or α_6 integrin (GoH3) reverted the M12 cells back to smooth acini-like structures, whereas IgG had little affect (Fig. 5A). Similar treatment of the F6 subline showed little difference, although there may be a slight reduction in acinus size. Immunostaining with the E-cadherin antibody showed that treatment with either AIIB2 or GoH3 restored some E-cadherin expression, resulting in some evidence of polarization akin to F6 acini structures (Fig. 5B, c_2 and c_4 compared with d_2 and d_4). Importantly, neither the AIIB2 nor the GoH3 antibody had an effect on F6 acini formation. Thus, this affect appears to be specific to M12 cells. Western blots showed that AIIB2 treatment did dramatically decrease β_1 integrin expression ($\approx$85%) in both M12 and F6 sublines, whereas vimentin expression in the M12 subline or actin levels in either subline was not affected (Fig. 5C). These results differed from other studies, where acinar formation of normal prostate epithelium was practically obliterated by the addition of either α_6 or β_1 blocking antibodies (18) but does agree with the fact that β_1 integrin is more associated with the formation of focal adhesion complexes involved with motility than stable hemidesmosomal attachment sites used more for the anchoring of cells. To our knowledge, this is the first time that the effect of α_6 and β_1 integrin function-blocking antibodies has been tested against metastatic prostate cells rather than normal prostate epithelial three-dimensionally, a more relevant assay for determining how changes in protein expression contribute to tumor progression.

Discussion

The analysis of relevant marker proteins (E-cadherin, keratins, β-catenin, and α_6 and β_1 integrins) in these genetically related, human prostate epithelial sublines grown in lrECM gels shows that the relative distribution and proportion of cell surface integrins controls the structural homeostasis of these cells. The parental P69 cell line produces structures that are morphologically similar to human glandular prostate epithelial cells (2). α_6 and β_1 Integrin expression is polarized in the P69, poorly tumorigenic F6, and M12-Vim acini, but polarization disappears in the disorganized mass of tumorigenic and metastatic M12 cells. The weakly tumorigenic LNCaP cell line displayed features of integrin polarization akin to P69, F6, or M12-Vim sublines, but the metastatic PC3 cell line formed solid spheroids of cells similar to initial M12 cultures. With time, the M12 subline grew out of such disorganized spheroids, which may reflect its highly metastatic phenotype (22). Thus, a thorough analysis of these P69-derived sublines has revealed *in vitro* morphologic properties, which correlate with their tumorigenic/metastatic behavior *in vivo* and to the more common LNCaP and PC3 prostate cell lines (21, 22). Overall, our results agree with those studies where an inverse relationship was found between acinar formation and malignancy (2, 36).

Recently, a correlation between vimentin expression and the degree of metastasis was confirmed in another set of genetically related prostate cells lines (37). More importantly, we found vimentin expression to be a crucial component of the morphologic changes observed by cells grown three-dimensionally. Disorganized M12 cells containing

vimentin did not form acini in lrECM gels but moved out of spheroids and spread throughout the matrix with little evidence of any acini structure. On the other hand, the P69 and F6 sublines express little vimentin but did form acini-like structure in lrECM gels. Blocking vimentin gene expression via shRNA reverted M12 cells to producing acini-like structures. These results imply that the lack of vimentin protein is essential for formation of acini-like structures by these sublines *in vitro*. M12-Vimcells displayed a considerable reduction in tumor growth *in vivo*, consistent with those morphologic differences displayed *in vitro*. Although several studies document a requirement for vimentin in motility and invasion assays *in vitro*, this is the first indication of such a dramatic effect on prostate tumor growth *in vivo* dependent on the continued expression of vimentin, although a similar role has been noted in breast and head and neck cancer cell lines (11–14, 38, 39).

An increase in β1 integrin expression has been found in actual prostate tumor samples as well as in more dedifferentiated tumor cells (3, 30). Similar results have been reported for metastatic mammary gland epithelial cell lines, where reversion by an inhibitory α_6 or β1 integrin antibody or its F(ab')2 fragment led to the reestablishment of E-cadherin-β-catenin complexes (40). In our study, the interruption of α_6 or β1 integrin expression reversed the morphologic phenotype of the metastatic M12 subline back to organized, polarized acini three-dimensionally as proposed but never proven experimentally (5). Although β1 integrin inhibitory antibodies were shown to block acini formation in a previous study, cells were plated on top of lrECM and had to first move into the gel to subsequently form acini, addressing a different experimental question than here (18). Our results suggest that α_6 or β1 integrin blocking antibodies could represent a relevant therapy to combat prostate tumor progression as has been suggested for metastatic breast cancer (41).

It has been postulated that, in motile cells, vimentin is responsible for moving endocytosed β1 integrin from the rear of the cell to the leading edge under the control of protein kinase C-ε (42). On inhibition of protein kinase C-ε and loss of vimentin phosphorylation, integrins become trapped in endocytic vesicles and directional motility toward the ECM is severely attenuated. Other studies proposed that vimentin functions as a carrier to move cargo on microtubules using kinesin/dynein motors (43). Although vesicle movement on the IFP network itself has never been documented, inhibitors that collapse microtubules affect the IFP network, suggesting cross-talk (43). Because the IFP network is the only filament that completely traverses the cytoplasm, a role in signal transduction has been proposed (44). Until now, the nature of the cargo carried by vimentin in nonneuronal cells was unknown. Based on our results and the literature, we propose that vimentin may contribute to moving β1 integrin to the leading edge to support motility in prostate carcinoma. Because α_6 integrin expression also correlates with a more metastatic phenotype and α_6 blocking antibodies reverted the morphology of the M12 subline, α_6 integrin may also play a role in prostate invasion (5, 30, 45, 46). Currently, we propose that vimentin- β1 integrin interaction is required for motility, an important precondition for establishing the metastatic property of M12 cells *in vivo*. Interrupting this movement by blocking α_6 and β1 integrin antibodies or reducing the amount of vimentin protein via shRNA interference reverted cells to acini-like structures

in vitro and severely reduced growth in nude mice. We propose that, by understanding the nature of the vimentin-integrin interaction, perhaps target molecule(s) could be generated to block this association. These molecules would be specific for the poorly differentiated, highly metastatic cell, because it is only this cell type that is motile and highly expresses both α_6 and β1 integrin and vimentin (19, 47). Such molecules may also present a relevant therapy for other poorly differentiated metastatic tumors such as breast, which also coexpress β1 integrin and vimentin at high levels (28).

In summary, growth of the P69, M12, and F6 sublines in lrECM gels presents a biologically relevant model system for determining what controls morphologic differences *in vitro* that contribute to promote tumor progression *in vivo*. It is anticipated that growth of these unique prostate sublines three-dimensionally will lead to the detection of relevant markers/targets that could be useful in the diagnosis, prevention, and ultimate treatment of prostate tumor progression. In addition, these sublines and the three-dimensional technology could be easily adapted to high-throughput screening for drugs, which could modify M12 morphologic behavior *in vitro* and identify a useful future therapy to counteract high tumor growth rates and/or metastasis *in vivo*.

Disclosure of Potential Conflicts of Interest

No potential conflicts of interests were disclosed.

Acknowledgements

We thank Frances K. White and the confocal imaging facility from the Massey Cancer Center (supported in part by NIH grant P30CA16059) and Dr. Davis Massey (Department of Pathology, Virginia Commonwealth University School of Medicine) for photography of immunofluorescence-stained tissue.

References

1. Barcellos-Hoff MH, Aggeler J, Ram TG, Bissell MJ. Functional differentiation and alveolar morphogenesis of primary mammary cultures on reconstituted basement membrane. Development 1989;105: 223–35.
2. Webber MM, Bello D, Kleinman HK, Hoffman MP. Acinar differentiation by non-malignant immortalized human prostatic epithelial cells and its loss by malignant cells. Carcinogenesis 1997;18:1225–31.
3. Murant SJ, Handley J, Stower M, Reid N, Cussenot O, Maitland NJ. Coordinated changes in expression of cell adhesion molecules in prostate cancer. Eur J Cancer 1997;33:263 –71.
4. Schmelz M, Cress AE, Scott KM, et al. Different phenotypes in human prostate cancer: α_6 or α_3 integrin in cell-extracellular adhesion sites. Neoplasia 2002;4:243–54.
5. Cress AE, Rabinovitz I, Zhu W, Nagle RB. The α6β1 and α6β4 integrins in human prostate cancer progression. Cancer Metastasis Rev 1995;14: 219–28. Molecular Cancer Therapeutics 507 Mol Cancer Ther 2009;8(3).March 2009
6. Cunha GR, Hayward SW, Wang YZ, Ricke WA. Role of the stromal micro-environment in carcinogenesis of the prostate. Int J Cancer 2003; 107:1–10.
7. Bissell MJ, Rizki A, Mian IS. Tissue architecture: the ultimate regulator of breast epithelial function. Curr Opin Cell Biol 2003;15:753–62.
8. Gilles C, Thompson EW. The epithelial to mesenchymal transition and metastatic progression in carcinoma. Breast J 1996;2:83–96.
9. Thompson EW, Newgreen DF, Tarin D. Carcinoma invasion and metastasis: a role for epithelial-mesenchymal transition? Cancer Res 2005;65:5991–5.
10. Tarin D, Thompson EW, Newgreen DF. The fallacy of epithelial mesenchymal transition in neoplasia. Cancer Res 2005;65:5996–6000.
11. Hendrix MJ, Seftor EA, Chu YW, Trevor KT, Seftor RE. Role of intermediate filaments in migration, invasion and metastasis. Cancer Metastasis Rev 1996;15:507 –25.
12. Gilles C, Polette M, Zahm J, et al. Vimentin contributes to human mammary epithelial cell migration. J Cell Sci 1999;112:4615–25.
13. McInroy L, Maata A. Down-regulation of vimentin expression inhibits carcinoma cell migration and adhesion. Biochem Biophys Res Commun 2007;360:109–14.
14. Paccione RJ, Miyazaki H, Patel V, et al. Keratin downregulation in vimentin-positive cancer cells is reversible by vimentin RNAi, which inhibits growth and motility. Mol Cancer Ther 2008;7:2898 –903.
15. Schmeichel KL, Bissell MJ. Modeling tissue-specific signaling and organ function in three dimensions. J Cell Sci 2003;116:2377–88.
16. Kleinman HK, McGarvey ML, Hassell JR, et al. Basement membrane complexes with biological activity. Biochemistry 1986;25:312 –8.
17. Streuli CH, Bissell MJ. Expression of extracellular matrix components is regulated by substratum. J Cell Biol 1990;110:1405–15.
18. Bello-DeOcampo D, Kleinman HK, Deocampo ND, Webber MM. Laminin-1 and α6 β1 integrin regulate acinar morphogenesis of normal and malignant human prostate epithelial cells. Prostate 2001;46:142 –53.

19. Lang SH, Sharrard RM, Stark M, Villette JM, Maitland NJ. Prostate epithelial cell lines form spheroids with evidence of glandular differentiation in three-dimensional Matrigel cultures. Br J Cancer 2001;85:590–9.
20. Bae VL, Jackson-Cook CK, Brothman AR, Maygarden SJ, Ware JL. Tumorigenicity of SV40 T antigen immortalized human prostate epithelial cells: association with decreased epidermal growth factor receptor (EGFR) expression. Int J Cancer 1994;58:721–9.
21. Bae VL, Jackson-Cook CK, Maygarden SJ, Plymate SR, Chen J, Ware JL. Metastatic sublines of an SV40 large T antigen immortalized human prostate epithelial cell line. Prostate 1998;34:275 –82.
22. Astbury C, Jackso n-Coo kCK, Culp SH, Paisley TE, Ware JL. Suppression of tumorigenicity in the human prostate cancer cell line M12 via microcell-mediated restoration of chromosome 19. Genes Chromosomes Cancer 2001;31:143–55.
23. Lee GY, Kenny PA, Lee EH, Bissell MJ. Three-dimensional culture models of normal and malignant breast epithelial cells. Nat Methods 2007; 4:359–65.
24. Liu X, Wu Y, Zehner ZE, Jackson-Cook CK, Ware JL. Proteomic analysis of the tumorigenic human prostate cell line M12 after microcellmediated transfer of chromosome 19 demonstrates reduction of vimentin. Electrophoresis 2003;24:3445–53.
25. Hagan M, Yacoub A, Dent P. Ionizing radiation causes a dosedependent release of transforming growth factor a *in vitro* from irradiated xenografts and during palliative treatment of hormone-refractory prostate carcinoma. Clin Cancer Res 2004;10:5724–31.
26. Zhang X, Diab IH, Zehner ZE. ZBP-89 represses vimentin gene transcription by interacting with the transcriptional activator, Sp1. Nucleic Acids Res 2003;31:2900–14.
27. Herrmann ME, Trevor KT. Epithelial-mesenchymal transition during cell culture of primary thyroid tumors? Genes Chromosomes Cancer 1993; 6:239–43.
28. Thompson EW, Paik S, Brunner N, et al. Association of increased basement membrane invasiveness with absence of estrogen receptor and expression of vimentin in human breast cancer cell lines. J Cell Physiol 1992;150:534–44.
29. Hendrix MJ, Seftor EA, Seftor RE, Trevor KT. Experimental coexpression of vimentin and keratin intermediate filaments in human breast cancer cells results in phenotypic interconversion and increased invasive behavior. Am J Pathol 1997;150:483–95.
30. Nagle RB, Hao J, Knox JD, Dalkin BL, Clark V, Cress AE. Expression of hemidesmosomal and extracellular matrix proteins by normal and malignant human prostate tissue. Am J Pathol 1995;146:1498–507.
31. Plymate SR, Tennant MK, Culp SH, et al. Androgen receptor (AR) expression in AR-negative prostate cancer cells results in differential effects of DHT and IFG-I on proliferation and AR activity between localized and metastatic tumors. Prostate 2004;61:276–90.
32. vanLeenders G, Gage WR, Hicks JL, et al. Intermediate cells in human prostate epithelium are enriched in proliferative inflammatory atrophy. Am J Pathol 2003;162:1529–37.
33. vanLeenders GJ, Aalders TW, Hulsbergen-van de Kaa CA, Ruiter DJ, Schalken JA. Expression of basal cell keratins in human prostate cancer metastases and cell lines. J Pathol 2001;195:563–70.

34. Abrahams NA, Bostwick DG, Ormsby AH, Qian J, Brainard JA. Distinguishing atrophy and high-grade prostatic intraepithelial neoplasia from prostatic adeno-carcinoma with and without previous adjuvant hormone therapy with the aid of cytokeratin 5/6. Am J Clin Pathol 2003;120:368–76.
35. Klezovitch O, Risk M, Coleman I, et al. A causal role for ERG in neoplastic transformation of prostate epithelium. Proc Natl Acad Sci U S A 2008;105:2105–10.
36. Bello-DeOcampo D, Kleinman HK, Webber MM. The role of α6β1 integrin and EGF in normal and malignant acinar morphogenesis of human prostatic epithelial cells. Mutat Res 2001;480-481:209–17.
37. Wu M, Bai X, Xu G, et al. Proteome analysis of human androgenindependent prostate cancer cell lines: variable metastatic potentials correlated with vimentin expression. Proteomics 2007;7:1973–83.
38. Eckes B, Dogic D, Colucci-Guyon E, et al. Impaired mechanical stability, migration and contractile capacity in vimentin-deficient fibroblasts. J Cell Sci 1998;111:1897–907.
39. Singh S, Sadacharan S, Su S, Belldegrun A, Persad S, Singh G. Overexpression of vimentin: role in the invasive phenotype in an androgenindependent model of prostate cancer. Cancer Res 2003;63:2306–11.
40. Weaver VM, Petersen OW, Wang F, et al. Reversion of the malignant phenotype of human breast cells in three-dimensional culture and *in vivo* by integrin blocking antibodies. J Cell Biol 1997;137:231–45.
41. Park C, Zhang H, Pallavicini M, et al. β1 Integrin inhibitory antibody induces apoptosis of breast cancer cells, inhibits growth, and distinguishes malignant from normal phenotype in 3D cultures and *in vivo*. Cancer Res 2006;66:1526–35.
42. Ivaska J, Vuoriluoto K, Huovinen T, Izawa I, Inagaki M, Parker PJ. PKCq-mediated phosphorylation of vimentin controls integrin recycling and motility. EMBO J 2005;24:3834–45.
43. Helfand BT, Chang L, Goldman RD. Intermediate filaments are dynamic and motile elements of cellular architecture. J Cell Sci 2004; 117:133–41.
44. Helfand BT, Chou Y-H, Shumaker DK, Goldman RD. Intermediate filament proteins participate in signal transduction. Trends Cell Biol 2005; 15:568–70.
45. Rabinovitz I, Nagle RB, Cress AE. Integrin α6 expression in human prostate carcinoma cells is associated with a migratory and invasive phenotype *in vitro* and *in vivo*. Clin Exp Metastasis 1995;13:481 –91
46. Edlund M, Miyamoto T, Sikes RA, et al. Integrin expression and usage by prostate cancer cell lines on laminin substrata. Cell Growth Differ 2001; 12:99–107.
47. Lang SH, Hyde C, Reid IN, et al. Enhanced expression of vimentin in motile prostate cell lines and in poorly differentiated and metastatic prostate carcinoma. Prostate 2002;52:253–63

Figures

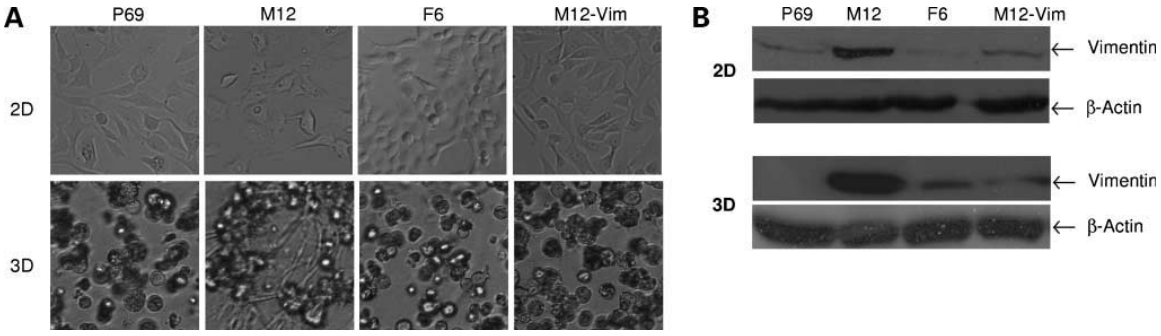

FIGURE 1

Comparison of the morphology of P69, M12, F6, and M12-Vim prostate sublines grown on tissue culture dishes (two-dimensional) versus embedded in lrECM gels (three-dimensional). **A**, light microscopy images of these various prostate cancer sublines were taken from cultures grown twodimensionally on traditional plastic dishes for 4 versus 8 days embedded in lrECM (three-dimensional) as described in Materials and Methods. Magnification, x10. **B**, whole-cell extracts (40 μg) from two- and three-dimensional cultures of these sublines were subjected to Western blot analysis with vimentin antibody as described in Materials and Methods. β-Actin was used as loading control.

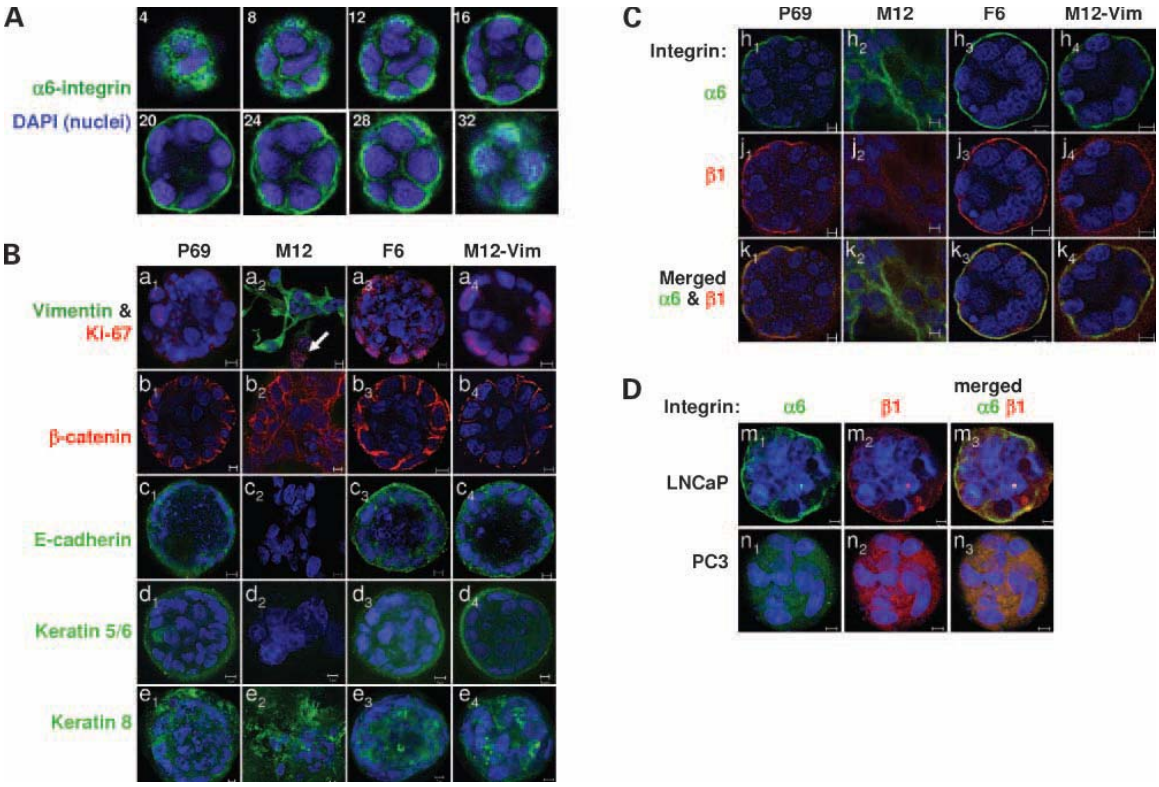

FIGURE 2

Comparison of content and localization of relevant proteins within the various morphologic structures formed by the P69, M12, F6, and M12-Vim prostate sublines grown embedded in lrECM gels. **A**, Z-stack of P69 acini from day 8 three-dimensional cultures was examined by immunofluorescence confocal microscopy. These eight pictures represent planes 4, 8, 12, 16, 20, 24, 28, and 32 from 40 such planes. Acini were fixed and stained with antibody to α_6 integrin (green). Nuclei were counterstained with 4',6-diamidino-2-phenylindole (blue) as discussed in Materials and Methods. Magnification, x 63. **B**, confocal immunofluorescence microscopy of structures formed by the various sublines at day 8 in lrECM stained with antibodies to vimentin (green) and Ki-67 (red; a_1-a_4), β-catenin (red; b_1-b_4), E-cadherin (green; c_1-c_4), keratin 5/6 (green; d_1-d_4), keratin 8 (green; e_1-e_4), and nuclei (blue) in all panels. **C**, cellular structures were stained with antibodies to α_6 integrin (green; h_1-h_4) or β_1 integrin (red; j_1-j_4) with overlay of $\alpha_6\beta_4$ integrin (k_4). For details of immunostaining, see Materials and Methods. **D**, LNCaP and PC3 cell lines were grown in lrECM and stained at day 8 as described in **C**. Bar, 5 μm (**B**-**D**).

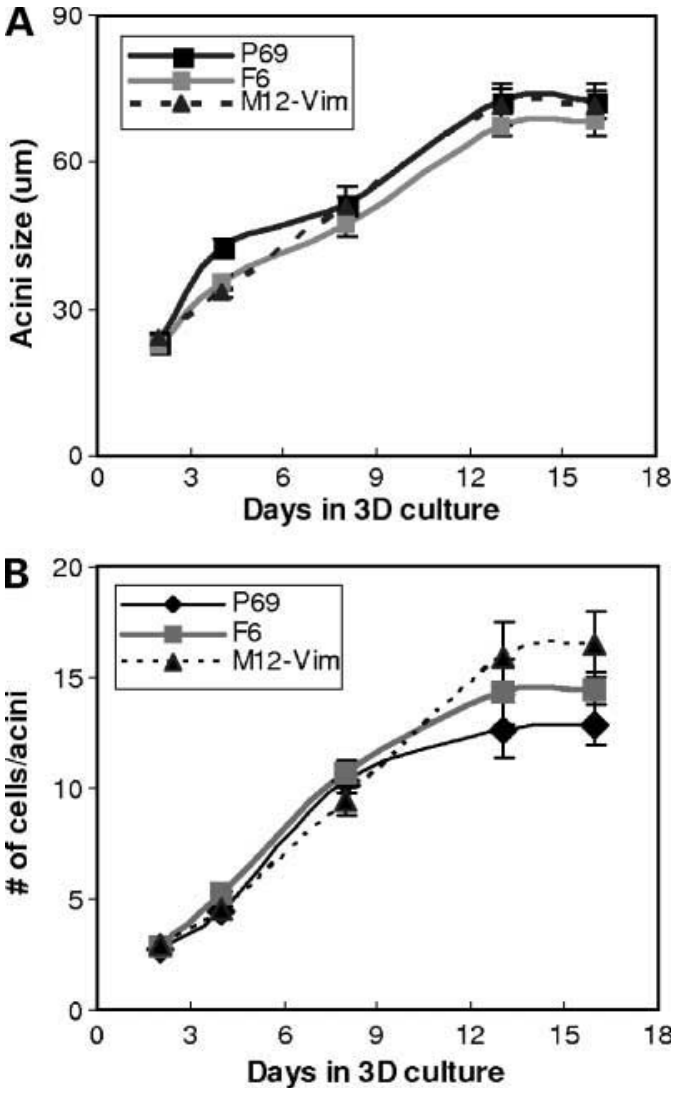

FIGURE 3

Growth properties of P69, F6, and M12-Vim acini in threedimensional culture. **A**, acini were isolated from P69, F6, and M12-Vim cultures grown embedded in lrECM gels for 2, 4, 8, 13, and 16 days. The average cell number per acini cross-section (from at least 100 acini) was counted using confocal microscopy. *Bars*, SE. B, average size of (Am) of acini (from at least 25 acini) was measured as in **A**. *Bars*, SE.

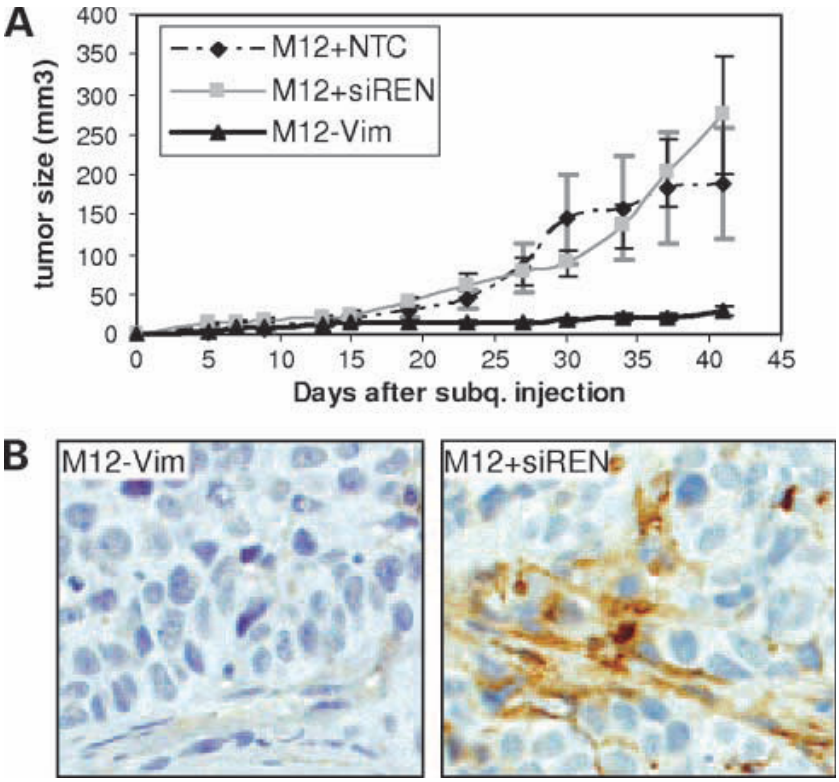

FIGURE 4

Tumorigenic properties of M12-Vim cells are reduced in athymic mice. A, tumor formation following s.c. injection of 1 x 10^6 M12-Vim cells (6 mice) was compared with the injection of cells containing vector-only M12+siREN (4 mice) or M12+NTC, a nontargeting RNA control (5 mice). Tumor growth was monitored by caliber measurement each 4 to 5 days for up to 42 days. All animals displayed tumors albeit of varying size and tumor volume (mm^3), calculated as described in Materials and Methods. *Bars*, SE. **B**, immunofluorescence staining with human vimentin antibody of paraffin-embedded M12+siREN (*left*) and M12-Vim (*right*) tumors retrieved from nude mice at time of euthanasia (42 days). Magnification, x400.